# Classification of Diabetic Foot Thermal Images Using Deep Convolutional Neural Network

**Reem N. Yousef[1*], Marwa M. Eid[2], Mohamed A. Mohamed[3]**

[1, 2] Delta Higher Institute for Engineering and technology, Mansoura, Egypt

[3] Electronics and communications Engineering, Faculty of Engineering, Mansoura University, Egypt

Emails: reem.nehad@hotmail.com; marwa.3eeed@gmail.com; mazim12@yahoo.com

**Abstract**

Diabetic foot (DF) is one of the most common chronic complications of poorly controlled diabetes mellitus (DM). Early diagnosis of DF and effective treatment is usually difficult by traditional approaches. Lately, it has been found a strong relationship between temperature variation and diabetic foot ulcer emergence. Thus, the current study focused on monitoring the temperature of feet using thermal images and its analysis techniques. The proposed system was based on employing a deep convolutional neural network (CNN) on thermal foot images. Experimental results showed that the proposed CNN has a maximum accuracy of 99.3% with minimum losses. When comparing the proposed system to other relevant systems, the proposed system approved greater accuracy, lower elapsed and testing time, which offers an automatic diagnostic tool for the diabetic foot and differentiates between its types. Thus, a simple, cost-effective, and accurate computer aided design (CAD) system could be presented to get a valuable system for the clinicians in hospitals.

**Keywords:** Diabetic Foot; Diabetes mellitus; convolutional neural network; Thermal images.

## 1. Introduction

For the header and the footer, just change the journal name and the abbreviation, then leave all other information for our production team at the ASPG editorial office to be updated after your paper acceptance. Diabetic foot disease is considered one of the most critical problems around the world. The delay in diabetic foot treatment may lead to devastating consequences, such as deep ulcers, infections, and partial or total amputation. The other problem represented in the dramatic increasing in number of diabetic patients, which is expected to exceed 500 million cases by 2030 compared to 350 million cases nowadays. It is worth mentioning that most of those patients are developing countries residents due to limited health care facilities and poor awareness [1]. The complications of the diabetic foot can be avoided by early diagnosis and appropriate treatment. In addition, there is not an automated system for early diagnosis of diabetic foot and differentiate between its types. In the recent years, studies revealed that there is a strong relation between temperature and diabetic foot ulcers emergence [1]. Many devices are available for measuring temperature of spots points such as liquid crystal thermography (LCT) [2], handheld dermal IR thermometers, temperature sensors integrated into a weighing scale [2], and infrared images.

Classical thermal statistics can be obtained by measuring the temperature of ROI points from the FLIR tools software then compute the absolute temperature difference between them. However, this method is not automated system, as it not able to differentiate between all types of complications under investigation. In current clinical practice, the proposed system can be used for distinguishing between the healthy and diabetic foot, then, differentiating its type according to Saint Elian Wound Score System (SEWSS) [3]. Deep convolutional neural network (DCNN) is used in thermal feet images classification to increase the accuracy value and decrease the learning time. The process of convolution in CNN also can extract relevant information at a low computational cost. The

advantages of using DCNN in early diagnosis of the DF don't stop on this limit only, but employing it in DF classification offers accurately, quickly, and immediate diagnoses without any faulting made by the manually selection of the points of region of interest (ROI) in the statistical thermal system. The proposed system also, doesn't need a specialist in diagnosis, owing to; it has ability of diagnosis DF automatically. The database of thermal images was collected by FLIR ONE thermal camera and an Android smartphone under specific conditions. The proposed image processing system was built depending on CNN image classification which had superior advantages comparing to machine learning (ML) [4] and the classical thermal statistics system. The results showed that the proposed CNN achieved the maximum accuracy, on comparing to conventional thermal statistics and machine learning [5]. Thus, the proposed system outperformed machine learning and conventional thermal statistics [6], [7] which lack important information about the shape and size in differentiating between diabetic foot cases with high level of accuracy.

The remainder of this paper was organized as follows: in the next section, there will be a description of the related works of diabetic foot thermal images. Section III provided detailed information about data acquisition system materials and methods. Section IV introduced data about the proposed system. Section V presented the results and discussion. Finally, conclusions and future work were given in the final.

## 2. Related Work

It is well known that to get an optimal solution for any linear programming problem using the direct simplex algorithm should be processed to be in standard form, the simplex method for solving an LP problem requires the problem to be expressed in the standard form. But not all LP problems appear in the standard form. In many cases, some of the constraints are expressed as inequalities rather than equations; Early diagnosis of the diabetic foot using thermal images is a promising modality of avoiding its devastating consequences, so there are many researches focused on the disease. H.Peregrina-Barreto et al. [6] detected the abnormality of the diabetic foot using thermal image by associating between temperature and its color code. In this method, the authors used a rainbow palette and segments it into ten colors the difference between each one 1℃. L. Vilcahuaman et al. [1] proposed a thermal system for detecting diabetic foot type II by automatic feet segmentation from a background using Chan and vese active contour method and then the authors applied rigid registration method. Finally, the absolute mean temperature difference between both feet had been computed. Their study was focused on detection of diabetic foot at hyperthermia only.  Image analysis algorithms in [5] were used to diagnose the diabetic foot. This study gave the largest classification accuracy till now of 95.66% to distinguish between normal and abnormal cases only. P. Sun et al. [8] used thermal feet images in differentiating between diabetic foot with and without sympathetic skin response by measuring a temperature of ROI points, then computing the mean temperature difference between corresponding areas on contralateral feet. C. Lui et al. [9] conducted studies using thermal images to detect diabetic foot abnormality as the following; segmenting thermal feet's from a background, then using non-rigid landmark-based registration B-splines to align both feet in the same position and detecting abnormality by comparing the temperature of the corresponding areas. However, cases with low risk of complication were not addressed in the current study and the only focus was on a group of high-risk diabetic patients that showed significant asymmetries between the left and right feet. M. Goyal et al. [10] applied different types of convolutional neural network to detect diabetic foot ulcer and they achieved the largest accuracy of 92.5%. Their study was interested in detect diabetic foot ulcer only. G. Serbu [7] proposed a system that can diagnose a diabetic foot using thermal images by computing the temperature of corresponding points in both feet's. The result declared that the average temperature in neuropathy patients was 32.8 ℃ and 27.9 ℃ in diabetic patients without neuropathy. Infrared images were applied in [11] to differentiate between three different stages of a diabetic foot as the following; no visible sign, local lesions, and severe complications. This can be achieved by thermal statistics, but this study was lacking important information about the size and shape of the feet which, maybe negatively affect the classification accuracy. M. Adam et al. [12] presented the system to detect

diabetic foot using thermal images by extract the textural and entropy features from decomposed discrete wavelet transform and higher order statistics, the classification result declared that the identification rate 89.39% but this study hadn't exposure all diabetic foot types. Thus, the introducing an automated classification system to diabetic foot grades is still an open problem.

## 3. Materials and Methods

### A. Acquisition protocol

The applied acquisition protocol has been depended on several devices: FLIR ONE thermal camera, Samsung Note five smartphone, temperature and humidity sensor, Accu-Chek Active meter, a tripod, and Polyurethane foam as shown in Fig. 1.
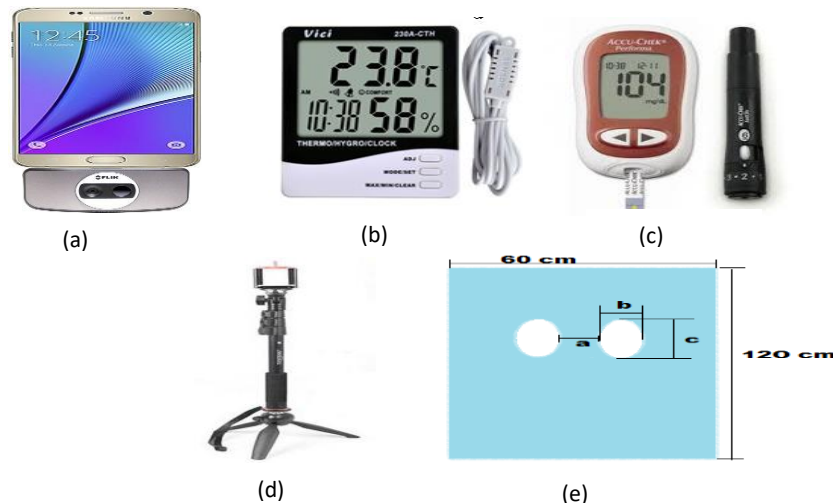


Figure 1: materials of data acquistion system (a) FLIR ONE thermal camera fixed on Samsung Note 5, (b) Sensor, (c) Accu-Chek Active meter, (d) tripod, (e) Polyurethane foam with dimensions a x c x b: 18 x 19 x 10 cm.

### B. Methods and conditions

The acquisition system protocol was started after a medical investigation, but the patient must take sufficient time to equilibrate with the ambient temperature, the room temperature must be well controlled within a range from 18 to 23°C, humidity (< 50%), and isolated from any external infrared radiation which affected on measurements. The elements of the system were arranged as shown in Fig. 2. Polyurethane foam was utilized to isolate feet from the rest of the body and ensure a homogenous background. The isolated surface must contain two holes, which suitable for passing through patient's feet it. They were two ellipses of 19 and 10 cm of two major axes each and separated by 18 cm. The isolated cover characteristics, tensile strength = 34.5-51.7 kPa, density =19.2 Kg/m3, of 120×60 cm, and 3 cm of thickness. The FLIR ONE thermal camera was chosen in acquiring dataset images. Its sensor is utilized as an IR detector that absorbs the infrared energy which was emitted from an object and then converts it into an electrical signal. IR is using the black body radiation law, presented by Max Plank, which states that any object with a temperature above zero converted to radiate body [6]. By following the black body radiation law, the human skin can be considered as a blackbody radiator, starting from using IR in medicine. Using this way, when the skin temperature changes, IR sensor captures the emitted radiation and then translates it to Thermo gram [6]. If the temperature of any region in skin increases or decreases, this region will emerge from the background. In the proposed system, FLIR ONE thermal camera can detect temperature in a range from -20 to 120 °C so it was able to distinguish between temperature differences in small values. It provided $480 \times 640$ pixels per frame at a rate of 60 frames per second. Each pixel had only temperature measurement value. So, it can easily differentiate between temperature pixel's values. FLIR ONE thermal camera specification is shown in                    Table **1** [13].

Table 1: FlIR ONE Camera Specifications

| Camera specification | Value |
|---|---|
| Temperature Measurement Range | -20° to 120°C |
| Field Of View (FOV) H×V | 46 × 35 ˚ |
| Detector Resolution | 160 × 120 pixel |
| Thermal Sensitivity | 0.1 ℃. |

## C. Subjects

The current study has been conducted from the 1st of July 2017 to the 30th of November 2017, with a population of healthy and diabetic volunteers. 50 participants were recruited from the Neuropathic Foot Clinic at Dar El Shefaa Hospital, Dakahlia Governorate, Egypt. These volunteers were divided into five groups, each group of 10 participants. Clinical history of participates, including age, gender, blood sugar level (BSL) and body mass index (BMI), were collected during the evaluation day. As shown in Table 2.



Figure 2: the proposed data acquisition system

The diabetic foot volunteers have been selected from patients to be in four different grades after a medical check which accordance with SEWSS. The SEWSS system has scored a better prediction tool of DF in [14] which make it more attractive to be depending on its classification. Each grade differs from the other in shape, size, and variance in colors between corresponding ROI points in both feet. For instance, in grade zero, the thermal images appear in a large variance in colors between corresponding ROI points and there are any foot disfigurements.

Table 2: Patients characteristics in accordance with SEWSS

| Patient Characteristics | | | | | | |
|---|---|---|---|---|---|---|
| Variables | Tot. | Risk | | | | |
| | | Norm | G 0 | G 1 | G 2 | G3 |
| Sample No. | 50 | 10 | 10 | 10 | 10 | 10 |
| Age (year) | 40/73 | 43/70 | 40/73 | 43/70 | 45/63 | 49/61 |
| Gender (F/M) | 32/18 | 6/4 | 7/3 | 5/5 | 7/3 | 6/4 |
| Weight (kg) | 47/130 | 47/95 | 75/120 | 71/95 | 70/130 | 69/121 |
| Height (cm) | 145/172 | 149/163 | 150/165 | 152/175 | 150/172 | 155/170 |
| BMI (kg/m²) | 16.1/50 | 16.1/36 | 31/49.9 | 27.7/36 | 22.5/45 | 25/49.9 |
| BSL (mmol/L) | 56/390 | 56/151 | 57/205 | 95/390 | 110/384 | 95/227 |

Grade 1 refers to the patients who have superficial ulcers, grade two there was a deep ulcer reached to tendons, which called infected ulcer or Charcot's foot. Finally, grade 3 refers to there are partially or totally amputation in feet due to a diabetic. The last group is referring to healthy cases from the hospital nurses volunteers. Fig. 4 shows a sample of visual and thermal healthy feet image obtained using the applied acquisition image protocol. As seen in Fig. 3, the thermal feet clearly appear as different colors on a homogenous background.



(a)                    (b)                    (c)

(d)                    (e)
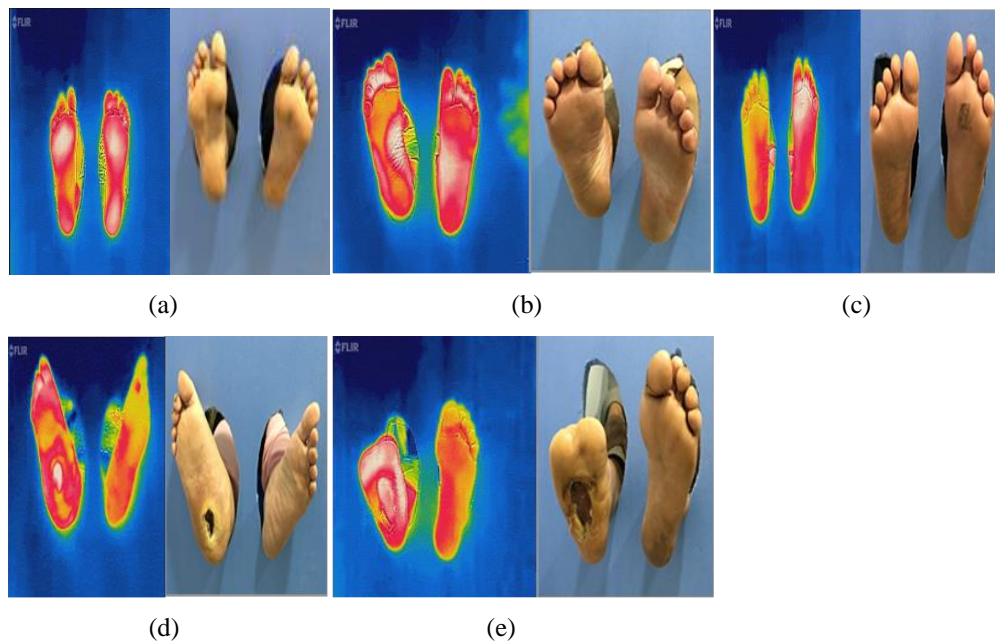
Figure 3: visual and thermal sample of dataset image, (a) normal case, (b) grade 0, (c) grade 1, (d) grade 2, and (e) grade 3 diabetic feet cases.

**D. Classical Thermal image analysis**

The thermal camera was stored images on a gray scale or a color spectrum. For each plantar image, the temperature of nine sub-regions of interest as in [8] had been measured using FLIR Tools software, including 1st, 3rd and 5th toe, 1st, 3rd and 5th distal metatarsal, 1st and 2nd lateral, and heel as shown in Fig. 4.
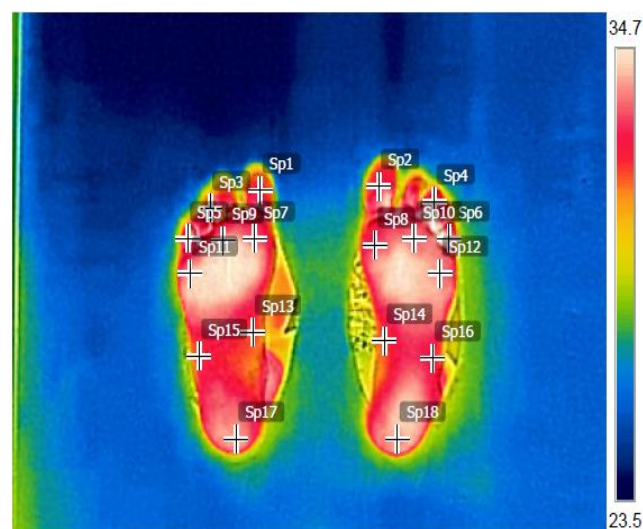


Figure 4: Thermal image temperatures results from FLIR

The temperatures values were then recorded in excel worksheet and finally, the mean absolute temperature differences between corresponding points are computed manually. The mean temperature difference ($\Delta T$) >1.5 °C between the ipsilateral and the contralateral foot referred to grade zero as in [15] diabetic foot, $\Delta T$ >2 °C refers to grade 1, $\Delta T$ >3 °C referred to grade 2 as in [11], and in case of there is any amputation in the insole this refers to grade three diabetic feet. The diagnosis using this method is not easy in all cases of the diabetic foot because it gives low accuracy, Moreover, diagnosis by this method depending on manual selecting ROI points and lack information about the shape and size of the affected feet.

## 4.   The Proposed System

Image classification using CNN's as an alternative to thermal analysis, is the most suitable choice of classification techniques. There are some problems still found in a dataset such as malleolus bone, unwanted clothes, shifting, and transition, according to this; these problems will be cured in the following preprocessing results steps. The acquired thermal images are analyzed as shown in Fig. 5, and passed through the following steps: (i) preprocessing to get rid of problems from gray thermal images, (ii) segmentation to isolate feet's from a background and then fit them in the same size of a network, and (iii) image classification using CNN's to identify each class.
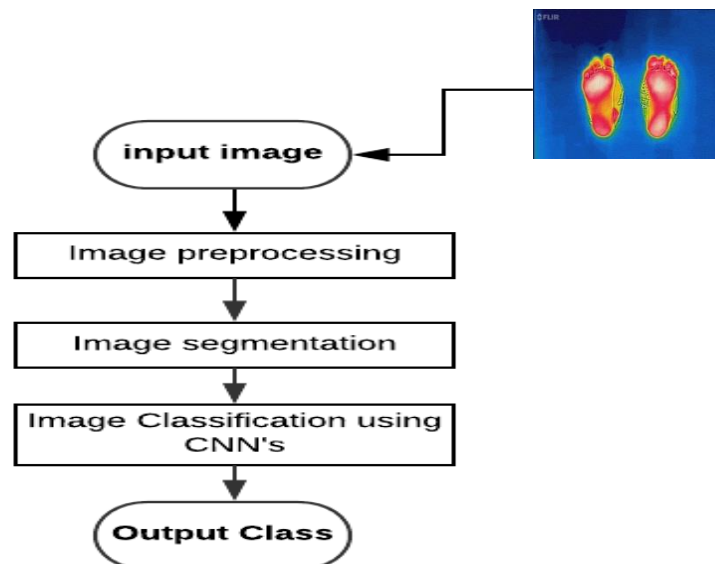


Figure 5: Thermal image analysis steps.

### A.   Image preprocessing

The input thermal image size is 480×640 pixels, these images should be isolated from back ground to get rid of problems which were caused by changing in patient foot's position, shifting, rotation, malleolus bone, and unwanted clothes. The mentioned problems were appeared due to, patient feet's moving during data acquisition system, these drawbacks will have a negative effect on the system performance and can decrease the differentiation accuracy. Thus, these problems will be eliminated as the following flowchart steps shown in Fig. 6.

The proposed pre-processing process is summarized in seven steps are involved:

- Step 0: converting all thermal images to gray scale.
- Step 1: creating feet mask using Gaussian Otsu threshold.
- Step 2: filling mask holes.
- Step 3: applying active contour on mask.
- Step 4: isolating feet from background by subtracting gray scale image from mask.

- Step 5: eroding segmented images.
- Step 6: using zero center technique to normalized and centralized them.
- Step 7: resizing output images to fit them to the same size of CNN's using data augmentation.

In the previous steps, the thermal images were converted into gray scale to minimize the elapsed time and facilitate the segmentation process. A Gaussian Otsu threshold [16] was then applied on the gray scale image to automatically create a feet mask and fill this mask based on morphological reconstruction [17]. Active contour [18] was used to smooth the mask edges by 500 iterations using trial and error method to reach the best smooth one. To obtain the segmented image, the gray scale images were subtracted from the masks which created in the first part of preprocessing. The segmented images were eroded using morphological operation [17] to shrink edges. Finally, the zero-center technique was normalized and centralized all images, and data augmenter was resized them in the same size of CNN's which are used. A sample of preprocessing results is shown in Fig.7.
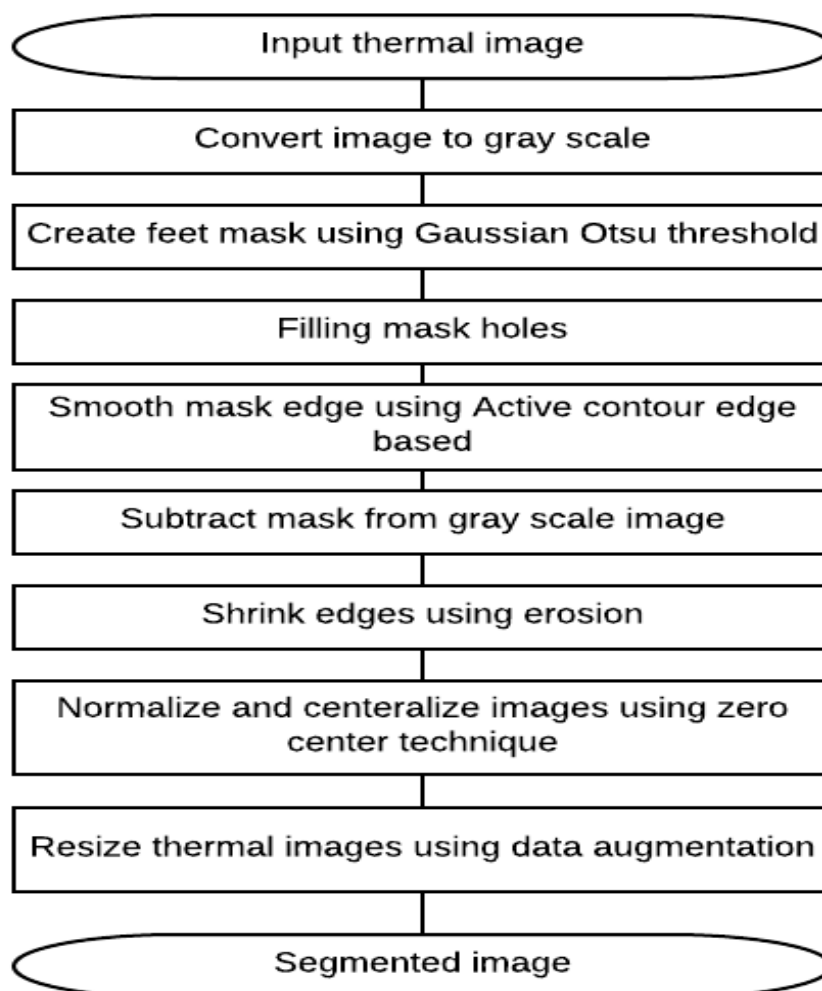


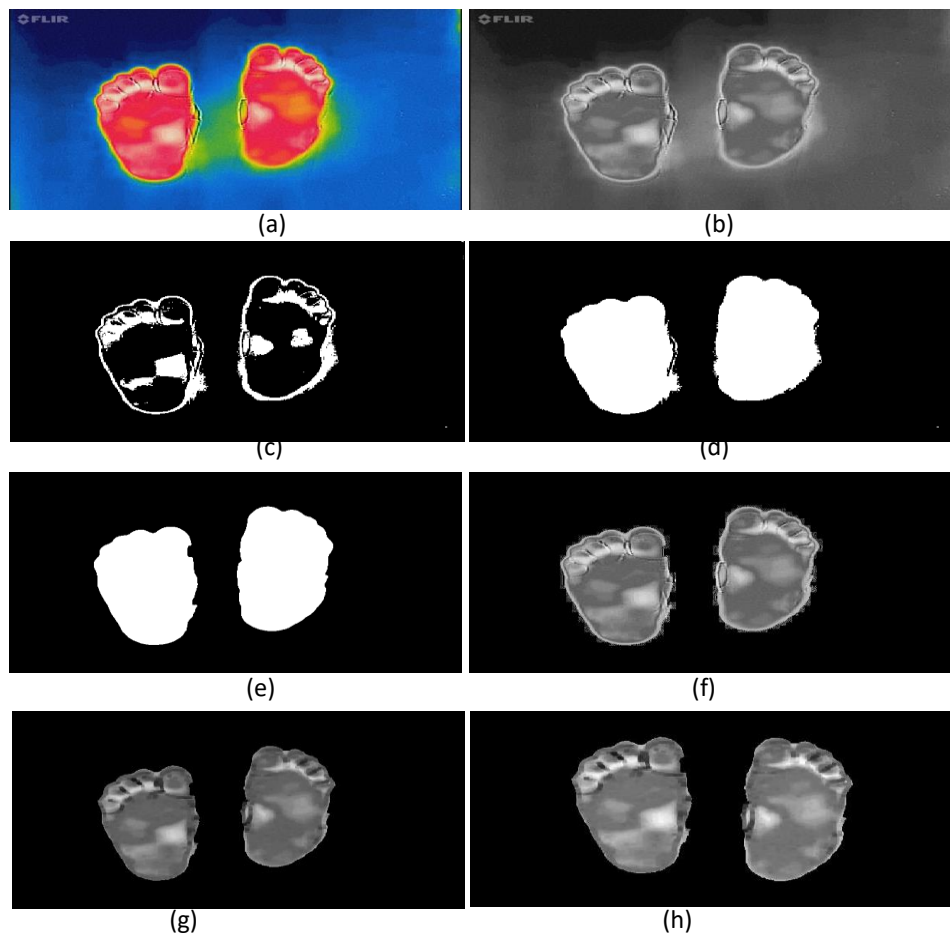Figure 6: Flowchart of the proposed preprocessing technique.

Figure 7: Sample of the preprocessing stage results,  (a) thermal image, (b) gray scale image, (c) Results of Gaussian  Otsu image, (d) filling mask, (e) active contour mask image, (f) gray scale after subtraction, (g) erode image, and (h) segmented image.

### B.   Classification Using Convolutional Neural Network

Lately, the demand for using automated systems increased instead of human efforts, especially when the machine learning and artificial intelligence have been emerged. The artificial neural networks perform the same rule of the biological neural network inside a human brain to solve a given problem like the brain thinking [19]. The structure of a fully connected artificial neural network is shown in Fig. 8.
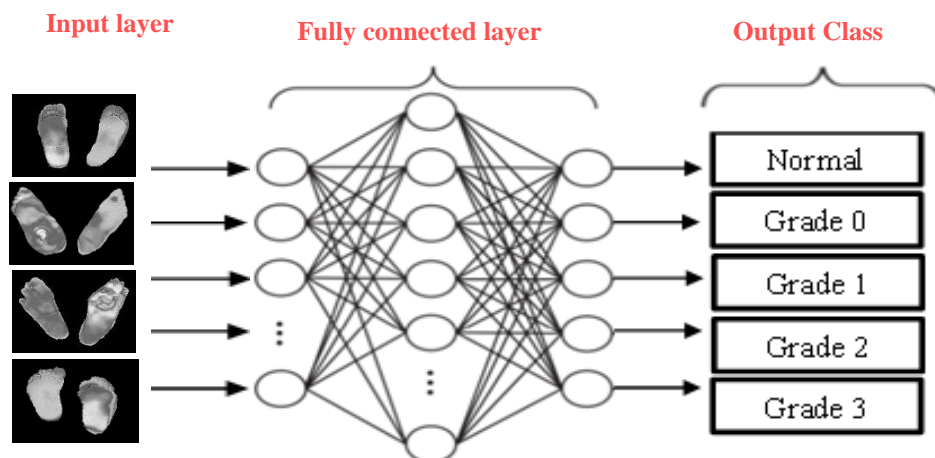


Fig. 8 Fully connected artifical neural network

Convolutional Neural Network (CNN) is a type of artificial neural networks, but its connections and parameters much fewer [20, 21]. Recently, by using the convolutional neural networks in image classification, the accuracy of performance can be improved, without extracting features from segmented images[22]. The convolutional Neural Network consists of some of the layers comprising both linear and nonlinear processes. These layers are learned in a joint modality [23]. The main blocks of any CNN are a convolutional layer, pooling layer, nonlinear Rectified Linear Units (ReLU) layer, fully connected layer, and the loss layer at the end [24], the structure of typical CNN shown in Fig. 9. CNN has also a large scale of applications such as visual tasks, natural language processing, image recognition, and classification. There are different types of CNN such as AlexNet, GoogLeNet, Vgg16, Vgg19, and resnet50 [25, 26], each type has its own structure, but the same building blocks. Any block has its main function. For instance; Convolution layers contain a rectangular matrix of neurons, pooling subsampling small rectangular blocks from the convolutional layer to reduce dimensionality, and Rectified Linear Unit (ReLU) can be used as an activation function to increase the nonlinear properties of the decision function. Finally, the fully connected layer takes all neurons in the previous layer then connects it to every neuron [27]. In the proposed system, AlexNet and GoogLeNet have been applied and their results are comparing with the proposed CNN.
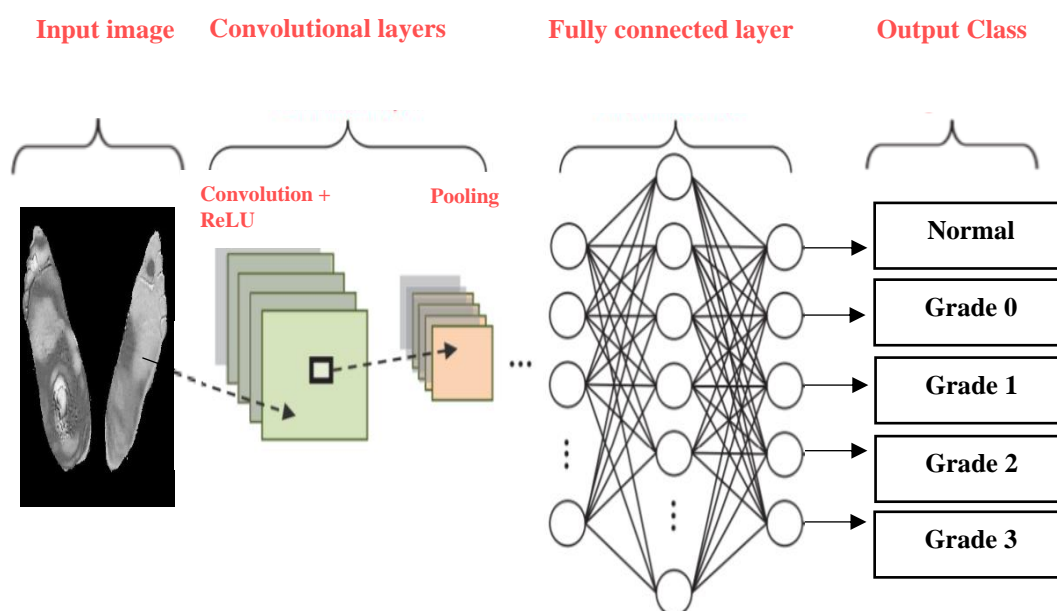


Figure 9:  The structure of typical convolutional neural network

### C.  The proposed Convolutional Neural Network

To improve the performance of classification results, a new convolutional neural network is introduced which called diabetic foot network (DFNET). Firstly, all thermal images in the dataset are resized to be 28×28×1 to reduce training time. DFNET is consists of 15 layer the first layer refers to the input layer. And the other layers are three convolutional layers with filter size 3×3 and number of filters is 16, 32, and 64 respectively. The normalization layer and nonlinear ReLU layer are stacked after each convolutional layer. In addition, the first and second convolutional layers are followed by max-pooling layers with size 2×2 and stride 2 to reduce the dimensionality. DFNET has the same values of convolutional layers filter size and pooling size with vgg16 and vgg19 [28] except the number of filters which have been doubled in each convolutional layer and chosen by trial and error to achieve a maximum classification accuracy value. The details of each layer of DFNET are shown in Fig. 10.
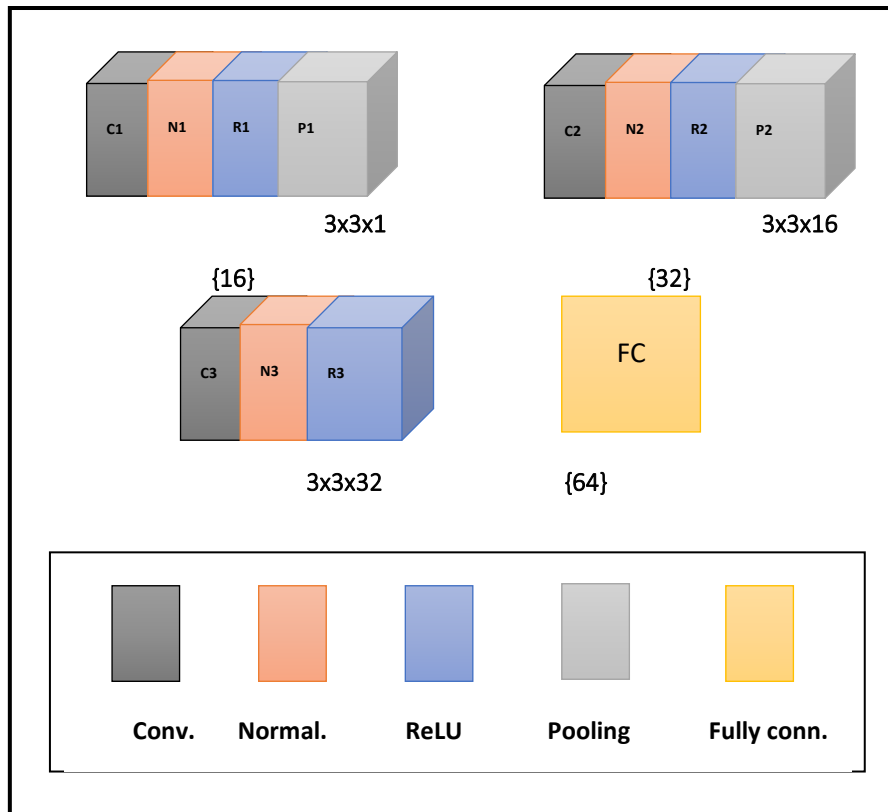
Figure 10: The proposed layers of DFNET

The parameters used for training with DFNET are 6 epochs, a batch size of 128, the learning rate of 0.01, a validation frequency of 30, and momentum 0.9. The detailed layers of the DFNET architecture are presented in Table 3. The output of each layer can be calculated by [29]:

$$L_{output} = \left[\frac{N - F + 2P}{S}\right] + 1 \tag{1}$$

Or

$$L_{output} = \left[\frac{N - F}{S}\right] + 1 \tag{2}$$

where, N is the input size, F is the filter or pooling size, P is the padding size, and S is the stride value. Eq. 1 computes the output layer with padding value. Eq. 2 computes the output in case of zero padding.

Table 3: The detailed layers of DFNET architecture

| Layer no. | Layer type | Filter size | Stride | Padding | Input | Output |
|---|---|---|---|---|---|---|
| Layer 1 | Conv. | 3×3 | 1 | 1 | 1×28×28 | 16×28×28 |
| Layer 2 | Max-pool. | 2×2 | 2 | 0 | 16×28×28 | 16×14×14 |
| Layer 3 | Conv. | 3×3 | 1 | 1 | 16×14×14 | 32×14×14 |
| Layer 4 | Max-pool. | 2×2 | 2 | 0 | 32×14×14 | 32×7×7 |
| Layer 5 | Conv. | 3×3 | 1 | 1 | 32×7×7 | 64×7×7 |

After the previous layer, fully connected layer (FC) refers to class probabilities. Thus, 5- class outputs of the DFNET as healthy, grade 0, grade 1, grade 2, and grade 3 diabetic foot patient are presented. The SoftMax layer (cross entropy) is the final layer and is described by [10],

$$f_j(z) = \frac{e^{z_j}}{\sum_k e^{z_k}} \tag{3}$$

where, $f_j$ is the $j^{th}$ element of the vector of class scores f and z is a vector of arbitrary real-valued scores.

## 5.  RESULTS AND DISCUSSION

The diabetic foot (DF) dataset was split into 70% training and 30% validation. In order to assess the performance of the proposed system, different important performance metrics were evaluated to confirm the robustness of the proposed system such as the elapsed time of training and testing phase, accuracy, sensitivity, false positive rate, precision, and F-score. The DFNET took an average 47 seconds for training, 14 seconds for testing time, and the other performance metrics are defined as follows:

Accuracy: is the number of correct predictions made divided by the total number of predictions made and calculated by [30]:

$$Accuracy = \frac{TP + TN}{TP + TN + FP + FN} \times 100 \tag{4}$$

Sensitivity: is the true positive rate (TPR) which measures the portions that are correctly classified and calculated by [31]:

$$TPR = \frac{TP}{TP + FN} \times 100 \tag{5}$$

where, TP is the true positive and FN is the false negative value.

False positive rate (FPR): is the fall-out value and it measures of incorrectly portions and can be defined as [30]:

$$FPR = \frac{FP}{FP + TN} \times 100 \tag{6}$$

where, FP is the false positive and TN is the true negative value.

Precision: is referring to positive predictive value (PPV) where it measures true positive value against positive value and it can be defined as [32]:

$$PPV = \frac{TP}{TP + FP} \times 100 \tag{7}$$

F-score: is measures a harmonic mean of precision and recall and can be calculated by [10],

$$F - score = \frac{2TP}{2TP + FP + FN} \times 100 \tag{8}$$

To evaluate the value of performance metrics, different important parameters were computed from the confusion matrix such as True Positive (TP), True Negative (TN), False Positive (FP), False Negative (FN), False Discovery Rate (FDR), and False Predictive Rate (FPR). The confusion matrix of DFNET is shown in Fig. 11.

Figure 11: Confusion matrix of DFNET

Using the previous performance equations, the detailed accuracy of applied DFNET classification is tabulated in Table 4.

Table 4: detailed accuracy of DFNET

| Class | Accuracy | TPR | FPR | PPV | F-score |
|---|---|---|---|---|---|
| **Normal** | 99.33 | 96.77 | 0 | 100 | 98.36 |
| **Grade 0** | 99.33 | 100 | 0.83 | 96.77 | 98.36 |
| **Grade 1** | 99.33 | 96.7 | 0 | 100 | 98.36 |
| **Grade 2** | 99.33 | 96.67 | 0 | 100 | 98.3 |
| **Grade 3** | 99.33 | 96.77 | 0 | 100 | 98.36 |
| **Average** | 99.33 | 97.4 | 0.166 | 99.35 | 98.35 |

Table 4 refers to the detailed accuracy of DFNET classification by the classes of fifth grades of diabetes and healthy participants. The patient classes were normal, grade 0, grade 1, grade 2 and grade 3. All classes scored the highest value of TPR with 100% correctly classified except grade 1. Accuracy of DFNET and loss curves is shown in Fig. 12.
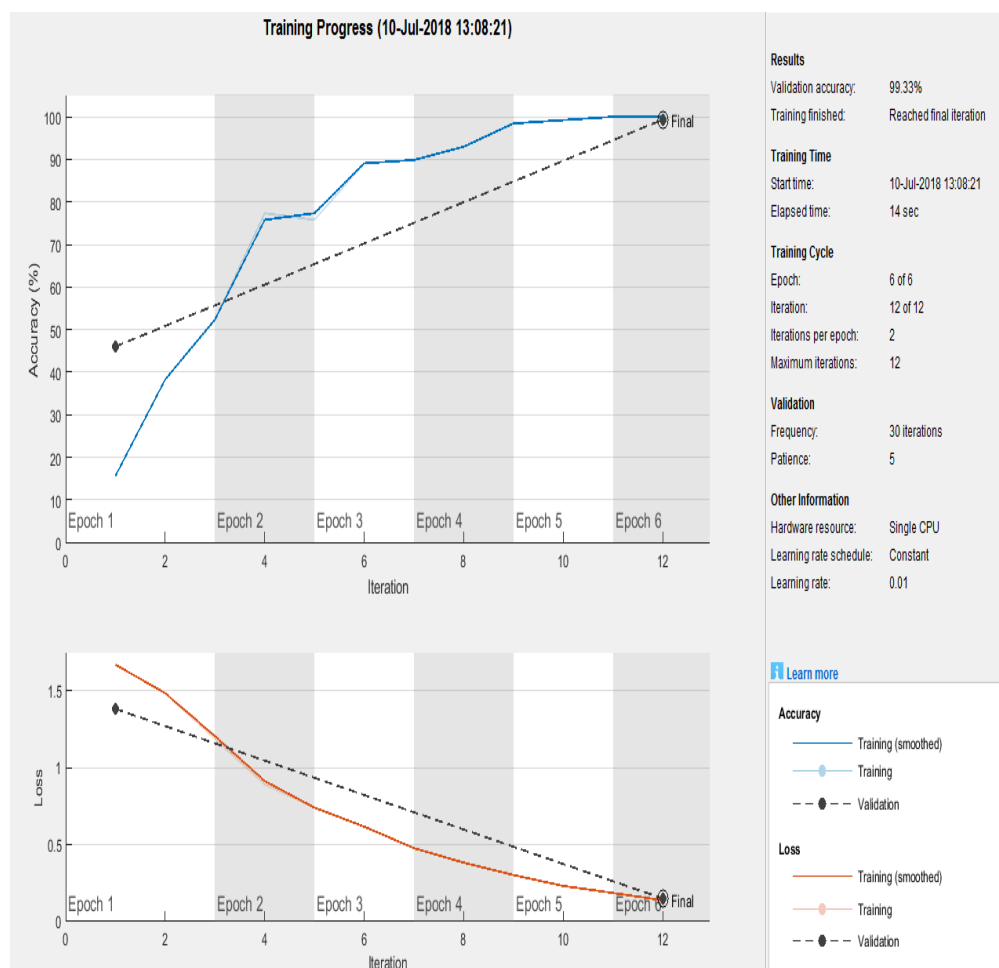
Figure 12: Accuracy and Loss curves of DFNET

In order to assess the performance of the proposed system, different types of CNN's are employed such as Alexnet and Googlenet after applying a few modifications on them to be compatible with the proposed dataset. Alexnet is one of the most famous deep CNN models, proposed by Alex Krizhevsky [23]. The original alexnet output must be changed to 5-class of participating instead of 1000 classes in the original network to work efficiently. Moreover, the parameters are used 6 epochs, a learning rate of 0.0001, a momentum of 0.9, a validation frequency of 30, and the minimum batch size 10. Further, the input image size must be changed to be 227×227×3 with the same size as the alexnet. Googlenet is presented by Szegedy et al. [33]. The fully connected value became 5 to classify the dataset into five classes. A momentum of 0.9; a batch size 10, a number of epochs is 6, validation frequency 30, and learning rate 10-4. The size of the images in the dataset was also adjusted to 224×224×3 with the same size as the googlenet. The classification results revealed that DFNET is better than the other systems, which scored 99.3% of the overall classification accuracy in 14 seconds elapsed time and training time is 47.53 seconds. When the proposed system was applied, the accuracy was enhanced by 5.64%, 7.93 % over using AlexNet and GoogleNet respectively. In DFNET, the result of classification accuracy is also, enhanced by 3.8% over using KNN in [5], and 11% over using SVM in [12] as shown in Fig. 13. The reason for increasing classification accuracy is using deep convolutional network instead of machine learning. So, the deep learning outperforms the machine learning in the classification problem. Accuracy also had been enhanced by 7.3% than DFUNET used in [10] as shown in Fig.13 and this reveals that the robustness of the proposed system. The classification accuracy results are shown in Fig. 13.
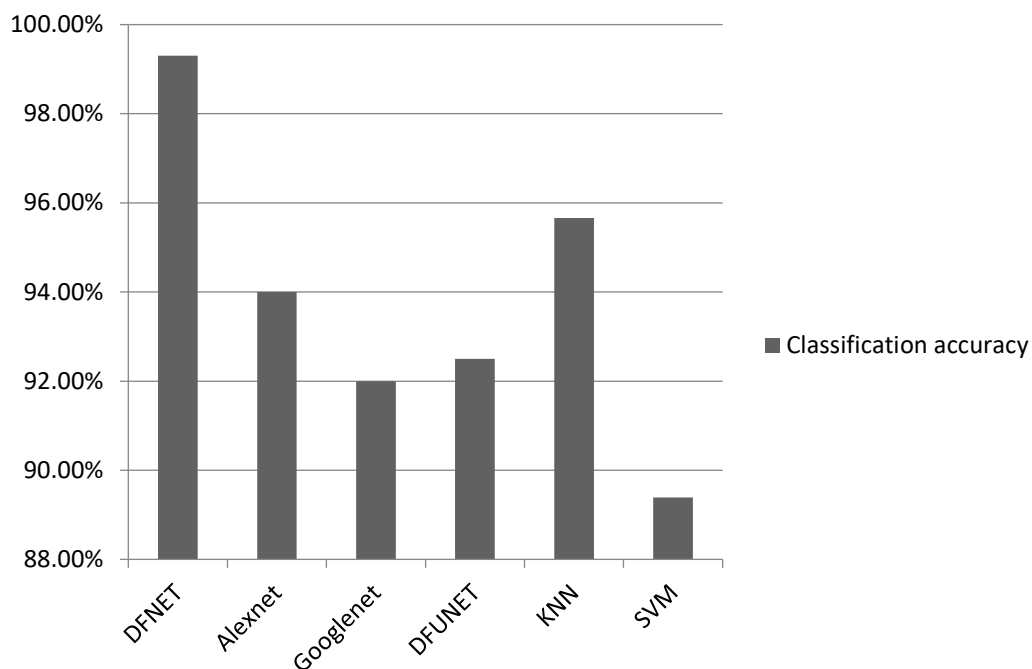
Figure 13: accuracy results of classifiers

The results of accuracy are presented in figure 13, proved that the proposed system is more accurate and efficient than another CNN's which are used and machine learning. Moreover, the DFNET may offer automatic medical diagnosis results with high accuracy and faster testing and lower casual errors owing to less human interventions. For testing, the applied DFNET took an average of 14 seconds whereas Alexnet took an average of 14 min and GoogLeNet took 15 min to classify the same test data. All tests were performed under Windows 10 (Microsoft Corporation) installed on an DELL LATITUDE E6410 personal computer with 4 GB internal working memory equipped with a Core i5 processor M520 (Intel Corporation) and 64-bit operating system. Thus, it could be more valuable to clinicians due to its capability of diagnosis and detection of diabetic foot type accurately and quickly.

## 6. Conclusion

In the proposed system, the dataset of thermal images had been collected by FLIR ONE thermal camera. Using thermal feet images, they induce of diabetic ulcer can be decreased. FLIR TOOLS software was used for measuring the temperature of ROI points, which helps in detecting the abnormality by computing the mean temperature difference between corresponding ROI points. Moreover, the proposed CNN technique was applied to the dataset for further analysis, to diagnose the abnormality, and identifying the diabetic foot type. When comparing the performance of different CNN classifiers, the DFNET offered the maximum classification accuracy and lesser probability of errors among the examined systems. To confirm the robustness of the DFNET system, its classification accuracy results were compared with the results of thermal statistics analysis, diagnosis which created by FLIR TOOLS software gave the same medical decision for each case. The proposed system were more advantageous than the traditional methods of thermal statistics analysis owing to, it's fastness, it offered automated diagnosis tool, and it has a capability to differentiate between diabetic foot types simply. The experimental results showed that using CNN as a classifier is better than the relevant systems in terms of the classification accuracy. In the future, it could be used in home regular checkup thanks to new technologies that recently appeared in mobile technologies and widely used it in hospitals to make the automatic diagnosis of a diabetic foot easier.

## References

[1] Vilcahuaman L, Harba R, Canals R, Zequera M, Wilches C, Arista M, et al., Automatic analysis of plantar foot thermal images in at-risk Type II diabetes by using an infrared camera. World Congress on Medical Physics and Biomedical Engineering, June 7-12, 2015, Toronto, Canada. Springer; 28-31, 2015.

[2] Roback K., An overview of temperature monitoring devices for early detection of diabetic foot disorders. Expert review of medical devices, 7(5), 711-718, 2014.

[3] Martínez-De Jesús FR., A checklist system to score healing progress of diabetic foot ulcers. The international journal of lower extremity wounds, 9(2), 74-83, 2010.

[4] Ahmed N. Al Masri , Hamam Mokayed, An Efficient Machine Learning based Cervical Cancer Detection and Classification, Journal of Cybersecurity and Information Management, Vol. 2, No. 2 , (2020) : 58-67 (Doi : https://doi.org/10.54216/JCIM.020203)

[5] Purnima S, Angelin.P S, Priyanka.R, Subasri.G, Venkatesh.R., Automated Detection of Diabetic Foot Using Thermal Images by Neural Network Classifiers. International Journal of Emerging Trends in Science and Technology, 4(5), 5183-5188, 2017.

[6] Peregrina-Barreto H, Morales-Hernandez LA, Rangel-Magdaleno J, Avina-Cervantes JG, Ramirez-Cortes JM, Morales-Caporal R., Quantitative estimation of temperature variations in plantar angiosomes: a study case for diabetic foot. Computational and mathematical methods in medicine, 2014.

[7] Serbu G, Infrared Imaging of the Diabetic Foot. Proceeding on InfraMation , 2009.

[8] Sun P-C, Jao S-HE, Cheng C-K. Assessing foot temperature using infrared thermography. Foot & ankle international, 26(10), 847-53, 2005.

[9] Liu C, van Netten JJ, Van Baal JG, Bus SA, van Der Heijden F, Automatic detection of diabetic foot complications with infrared thermography by asymmetric analysis. Journal of biomedical optics, 20(2), 2015.

[10] Goyal M, Reeves ND, Davison AK, Rajbhandari S, Spragg J, Yap MH. Dfunet: Convolutional neural networks for diabetic foot ulcer classification. arXiv preprint arXiv:171110448 2017.

[11] Van Netten JJ, van Baal JG, Liu C, van Der Heijden F, Bus SA. Infrared thermal imaging for automated detection of diabetic foot complications. SAGE Publications Sage CA: Los Angeles, CA, 2013.

[12] Adam M, Ng EY, Oh SL, Heng ML, Hagiwara Y, Tan JH, et al., Automated characterization of diabetic foot using nonlinear features extracted from thermograms. Infrared Physics & Technology, 89(3), 25-37, 2018.

[13] Fraiwan L, AlKhodari M, Ninan J, Mustafa B, Saleh A, Ghazal M., Diabetic foot ulcer mobile detection system using smart phone thermal camera: a feasibility study. Biomedical engineering online, 16(1), 2017.

[14] Huang Y, Xie T, Cao Y, Wu M, Yu L, Lu S, et al., Comparison of two classification systems in predicting the outcome of diabetic foot ulcers: the W agner grade and the S aint E lian W ound score systems. Wound Repair and Regeneration, 23(3), 379-385, 2015.

[15] Marques ARS. Diabetic foot thermophisiology characterization. 2014.

[16] Yousefi J. Image Binarization using Otsu Thresholding Algorithm. 2011.

[17] Gonzalez RC, Woods RE, Eddins SL. Morphological reconstruction. Digital Image Processing using MATLAB, MathWorks 2010.

[18] Airouche M, Bentabet L, Zelmat M., Image segmentation using active contour model and level set method applied to detect oil spills. Proceedings of the World Congress on Engineering. 1. Lecture Notes in Engineering and Computer Science, 1-3, 2009.

[19] Lu H, Li Y, Chen M, Kim H, Serikawa S., Brain intelligence: go beyond artificial intelligence. Mobile Networks and Applications, 23(2), 368-375, 2018.

[20] Vishal Dubey, Bhavya Takkar , P. Singh Lamba, Micro-Expression Recognition using 3D - CNN, Fusion: Practice and Applications, Vol. 1 , No. 1 , (2020) : 5-13. https://doi.org/10.54216/FPA.010101.

[21] Ahmed A. Elngar , Mohamed Arafa , Amar Fathy , Basma Moustafa , Omar Mahmoud , Mohamed Shaban , Nehal Fawzy, Image Classification Based On CNN: A Survey, Journal of Cybersecurity and Information Management, Vol. 6 , No. 1 , (2021) : PP. 18-50. https://doi.org/10.54216/JCIM.060102.

[22] Cheng G, Guo W., Rock images classification by using deep convolution neural network. Journal of Physics: Conference Series. 887. IOP Publishing, 012089, 2017.

[23] Elmahdy MS, Abdeldayem SS, Yassine IA., Low quality dermal image classification using transfer learning. Biomedical & Health Informatics (BHI). 2017 IEEE EMBS International Conference on. IEEE, 373-376, 2017.

[24] Spanhol FA, Oliveira LS, Petitjean C, Heutte L., Breast cancer histopathological image classification using convolutional neural networks. Neural Networks (IJCNN), 2016 International Joint Conference on. IEEE, 2560-2567, 2016.

[25] Condori RHM, Romualdo LM, Bruno OM, de Cerqueira Luz PH., Comparison between Traditional Texture Methods and Deep Learning Descriptors for Detection of Nitrogen Deficiency in Maize Crops. Computer Vision (WVC), 2017 Workshop of. IEEE, 7-12, 2017.

[26] Liu D, Wang Y. Monza, Image classification of vehicle make and model using convolutional neural networks and transfer learning, 2017.

[27] Abedallah Zaid Abualkishik , Ali A. Alwan, Multi-objective Chaotic Butterfly Optimization with Deep Neural Network based Sustainable Healthcare Management Systems, American Journal of Business and Operations Research, Vol. 4 , No. 2 , (2021) : 39-48. https://doi.org/10.54216/AJBOR.040203

[28] Simonyan K, Zisserman A., very deep convolutional networks for large-scale image recognition. arXiv preprint arXiv:14091556 2014.

[29] Murphy J., An Overview of Convolutional Neural Network Architectures for Deep Learning. 2016.

[30] Zhu W, Zeng N, Wang N., Sensitivity, specificity, accuracy, associated confidence interval and ROC analysis with practical SAS implementations. NESUG proceedings: health care and life sciences, Baltimore, Maryland,19-67, 2010.

[31] Hassan TM, Elmogy M, Sallam E-S. Diagnosis of focal liver diseases based on deep learning technique for ultrasound images. Arabian Journal for Science and Engineering, 42(8), 3127-3140, 2017.

[32] Hossin M, Sulaiman M., A review on evaluation metrics for data classification evaluations. International Journal of Data Mining & Knowledge Management Process, 5(2), 2015.

[33] Szegedy C, Liu W, Jia Y, Sermanet P, Reed S, Anguelov D, et al., Going deeper with convolutions. Proceedings of the IEEE conference on computer vision and pattern recognition,1-9, 2015.